LETTERS

A mechanism to thin the continental lithosphere at magma-poor margins

Luc L. Lavier[1] & Gianreto Manatschal[2]

Where continental plates break apart, slip along multiple normal faults provides the required space for the Earth's crust to thin and subside[1]. After initial rifting, however, the displacement on normal faults observed at the sea floor seems not to match the inferred extension[2]. Here we show that crustal thinning can be accomplished in such extensional environments by a system of conjugate concave downward faults instead of multiple normal faults. Our model predicts that these concave faults accumulate large amounts of extension and form a very thin crust (<10 km) by exhumation of mid-crustal and mantle material. This transitional crust is capped by sub-horizontal detachment surfaces over distances exceeding 100 km with little visible deformation. Our rift model is based on numerical experiments constrained by geological and geophysical observations from the Alpine Tethys and Iberia/Newfoundland margins[3–9]. Furthermore, we suggest that the observed transition from broadly distributed and symmetric extension to localized and asymmetric rifting is directly controlled by the existence of a strong gabbroic lower crust. The presence of such lower crustal gabbros is well constrained for the Alpine Tethys system[4,9]. Initial decoupling of upper crustal deformation from lower crustal and mantle deformation by progressive weakening of the middle crust is an essential requirement to reproduce the observed rift evolution. This is achieved in our models by the formation of weak ductile shear zones.

To allow the inclusion of mechanical decoupling of the upper crust and lower crust-mantle in numerical experiments, we propose a new formulation for the rheology of the crust (Fig. 1). Weakening associated with viscous strain accumulation has been included in previous numerical experiments and plays an important role in decoupling the upper crust from the lower crust and mantle[10]. However, studies in the Pogallo and Lugano–Val Grande shear zones in the Alps[11,12] and in other ductile shear zones (DSZs)[13,14] show that for polymineralic rocks, such as granite, localization occurs for high stress and low strain in the presence of fluids[9,15,16], and from low strain to high strain when the rock is transformed into a mylonite[17,18]. Hence, softening is both stress- and strain-dependent and causes a localized decrease in viscosity with respect to the surrounding rocks.

We chose to parameterize ductile softening as though it were governed by a decrease in viscosity from plagioclase to wet quartzite rheology[19] (Fig. 1c). The softening transition occurs only between the temperatures corresponding to the onset of quartz plasticity (300 °C) to that of plagioclase plasticity (450 °C). The transition occurs when the product of the effective stress σ^{eff} with the total accumulated strain $\varepsilon_{\mathrm{t}}^{\mathrm{eff}}$ is greater than 4×10^6 J (which is an approximate measure of the minimum work done to deform the system) (Fig. 1c) with $\sigma^{\mathrm{eff}} = \sqrt{(\sigma^{\mathrm{II}})}$ and $\varepsilon_{\mathrm{t}}^{\mathrm{eff}} = \sqrt{(\varepsilon_{\mathrm{t}}^{\mathrm{II}})}$ (where σ^{II} and $\varepsilon_{\mathrm{t}}^{\mathrm{II}}$ are the second invariants of the stress and strain). This was chosen to initiate an abrupt change in viscosity for stresses corresponding to the brittle–ductile transition (BDT) (100 MPa for the choice of the initial rheology) for 4% of strain. Deformation accumulates at the BDT where the upper, elastoplastic crust shears over the viscoelastic crust, and results in the formation of sub-horizontal ductile shear zones (Fig. 1d, e). In the example depicted in Fig. 1d, the DSZ is active at low angles (5°) near the BDT and the brittle fault is active at 45°. For higher strain (>20%), the stress needed to initiate ductile softening is of the order of a few tens of MPa or less (Fig. 1e). Thus, multiple, sub-horizontal DSZs will form in the vicinity of the 300 °C isotherm where the work criterion is satisfied. Our new parameterization also causes the deformation to follow the thermal evolution in the crust. As these DSZs become highly strained, they further weaken and form a wide, viscous channel. This rheological transition is critical in controlling the evolution of rifting.

Observations of the sediment, basement and fault architecture of the Alpine Tethys and Iberia/Newfoundland margins enable a precise description of the temporal and spatial evolution of deformation during rifting[3,4]. The pre-rift conditions were estimated from: the stratigraphic record of the Alpine Tethys, the crustal-scale seismic section across the Iberia and Newfoundland margins, and the pressure–temperature–time path through the Ivrea lower crustal section and Malenco crust-mantle boundary[4,9]. These show that the pre-rift crust was ~30 km thick, dominated by quartzo-feldspathic upper and middle crust, and with a gabbroic lower crust inherited from post-Variscan extensional collapse in the Permian period (Fig. 1a). The temperature and pressure conditions at the crust–mantle boundary were 550 °C for 0.9–1.0 GPa at the onset of rifting[9] (Fig. 1a). The volcanic activity during rifting is lacking at both margins, arguing for a cold initial geotherm.

Using structural reconstructions, we identify three phases of rifting (Fig. 2a). The initial 'stretching mode', A, is characterized by distributed listric-normal faulting, cutting through the brittle upper crust and soling out at mid-crustal levels. The faults bound the rift-basins, up to 4 km deep and 30 km wide. Fault offsets are less than 10 km and total extension is limited. Both hanging wall and footwall are subsiding (A in Fig. 2a). The type examples are the Generoso basin in the Southern Alps[12] and the Jeanne d'Arc basin in Newfoundland[20].

The 'thinning mode', B, follows and affects the future distal margin in a narrow zone. This area of the margin is commonly buried under thick sediments. In seismic sections there is little evidence of upper crustal extension. Drill-holes are rare and do not provide much information about tectonic subsidence or the nature of the basement. From the Alps, pressure–temperature–time data from the Ivrea lower crustal section[21] can be related to fault activity along a major DSZ (for example, the Pogallo shear zone[21]) while the isostatic movements are constrained by the stratigraphic record exposed in the Briançonnais and Err/Canavese domains (B in Fig. 2a). These observations suggest the occurrence of crustal-scale shear zones thinning the crust to less than 10 km, without the presence of distributed normal faulting in

[1]University of Texas Institute for Geophysics, Jackson School of Geosciences, Austin, Texas 78759, USA. [2]CGS-EOST, Université Louis Pasteur, 1 rue Blessig, F-67084 Strasbourg, France.

the upper crust and associated large subsidence. Such crustal-scale shear zones were described for the Iberia margin[7] (for example, seismic reflector[4] C), whereas more accurate geological constraints were obtained from the Alps (for example, Pogallo fault[21]) (B in Fig. 2a). Other possible examples of the thinning phase are the Galicia Interior basin near Iberia[22] and the west African margin[23]. In all of these examples, thinning of the crust is accompanied by little or no evidence of upper crustal deformation.

The 'exhumation mode', C, is characterized by downward concave faults that generate fault offsets (more than 10 km) without producing major observable topography, because the subcontinental mantle is exhumed at the sea floor[3]. Examples of this fault system were seismically imaged and drilled in the Iberia abyssal plain[3] and are exposed in the Err and Platta nappes in the Alps[4] (C in Fig. 2a). Exhumed mantle in the ocean continent transition[5,6] is associated with late, shallow-crustal detachment systems[7–9], and is serpentinized at temperatures under 600 °C and at depths less than 10 km, where hydrothermal circulation is occurring[24].

The numerical experiments were performed with an extended version of the numerical code PARAVOZ[25]. We use initial conditions and a rheological parameterization derived from observations in the Alps (Fig. 1a). The lithosphere is modelled as a nonlinear viscoelastoplastic material[26]. The crust is initially 30 km thick. For the first 24 km, the rheology approximates the mechanical behaviour of a polymineralic material composed of plagioclase and quartz. The deepest 6 km of the crust is gabbroic and modelled with a nonlinear Maxwell viscoelastic rheology, which is intermediate between plagioclase (anorthosite) and dry olivine. The mantle is modelled as a dry olivine. The temperature at the crust–mantle boundary is taken to be 550 °C, increasing to 1,300 °C at 100 km depth, and is set at 10 °C at the surface.

The modelled extension follows the same evolution as that predicted by geological observations. It starts by the formation of distributed normal faults rooted in the middle crust and is weakened by the formation of several DSZs (A in Fig. 2b). The weak middle crust flows over the strong lower crust and allows for the

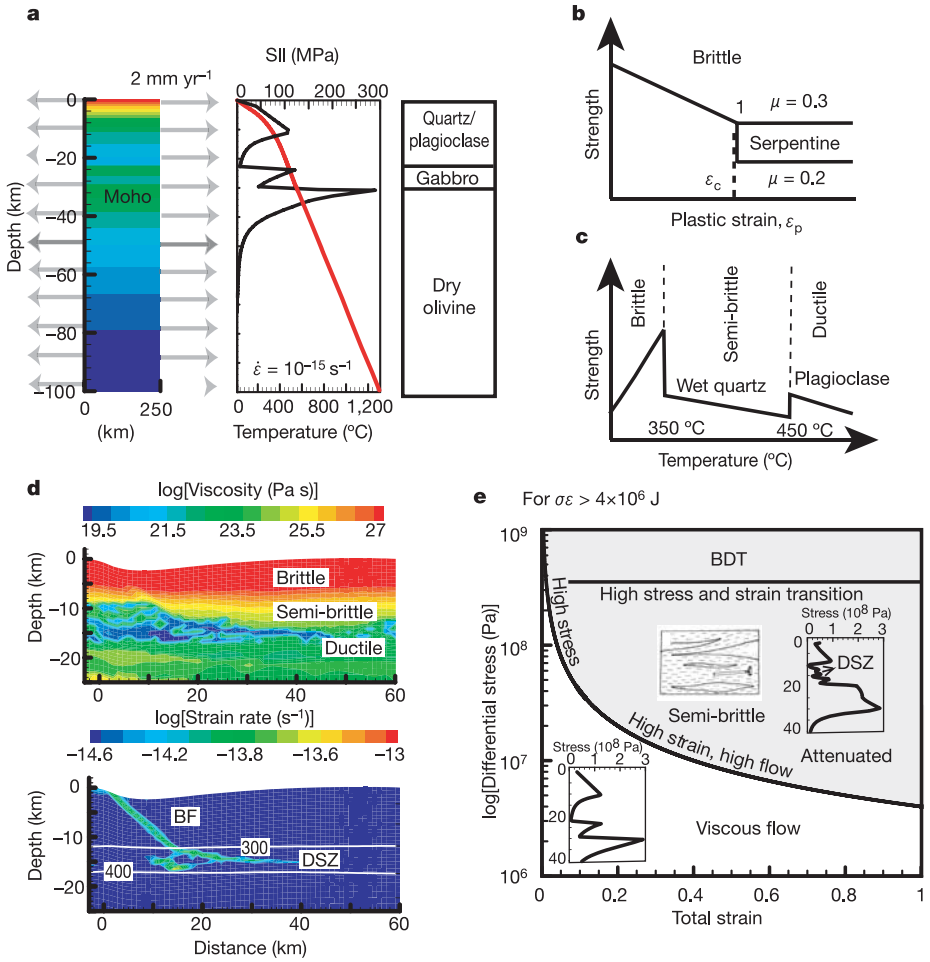

Figure 1 | Geological constraints, rheological parameterization and modelling approach. **a**, The sides of the model are pulled apart at a constant half-rate of 2 mm yr^{-1}. Isostatic equilibrium is simulated at the bottom while the top surface is stress-free to model the topographic evolution. SII is the yield stress. **b**, In the brittle areas, the lithosphere is elastoplastic with a Mohr–Coulomb yield criterion. The material is both frictional and cohesional (initially the friction coefficient $\mu = 0.6$ and the cohesion $C = 44$ MPa). Both cohesion and friction decrease locally as a function of plastic strain (10%) to trigger the formation of shear bands (to $\mu = 0.3$ and $C = 4$ MPa). Serpentinization occurs in the mantle for temperatures under 600 °C and depths under 10 km, and we further decrease the friction coefficient at this depth to 0.2 (ref. 29). Crustal and mantle density are 2,800 kg m^{-3} and 3,300 kg m^{-3} respectively. Power-law creep parameters are: crust, quartz[30] (exponent $n = 3$, activation energy $Q = 2 \times 10^5$ J mol^{-1}, pre-exponent $A = 5 \times 10^2$ MPa^{-n} s^{-1}) and plagioclase[31] ($n = 3.2$, $Q = 2.38 \times 10^5$ J mol^{-1}, $A = 3.3 \times 10^{-}$ MPa^{-n} s^{-1}), gabbroic lower crust ($n = 3.05$, $Q = 3.5 \times 10^5$ J mol^{-1}, $A = 1.25 \times 10^{-1}$ MPa^{-n} s^{-1}), mantle, dry olivine[32] ($n = 3$, $Q = 5.2 \times 10^5$ J mol^{-1}, $A = 7 \times 10^4$ MPa^{-n} s^{-1}). ε_c is the characteristic plastic strain for which the material has weakened. **c**, Schematic decrease in viscosity associated with the formation of a ductile shear zone. **d**, Viscosity and strain-rate fields for a listric normal fault. The brittle–plastic fault (labelled BF) roots at 12 km in a sub-horizontal low-viscosity layer (DSZ) extending down to 15 km between the 300 °C and 400 °C isotherms. **e**, Brittle to semi-brittle, semi-brittle to ductile, and brittle to ductile transitions in the stress–strain space for our parameterization.

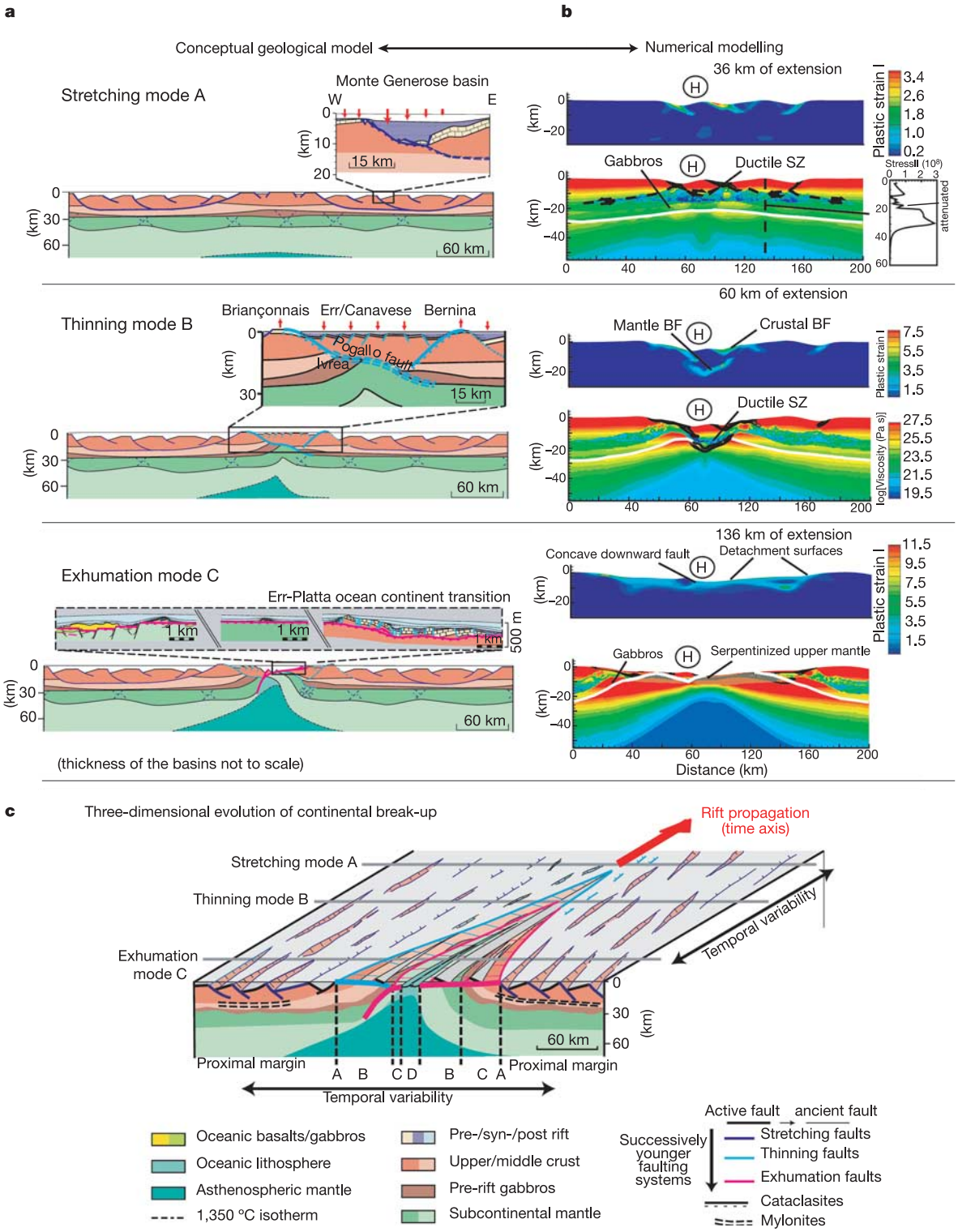

Figure 2 | Modes of extension leading to continental break-up and three-dimensional concept for the temporal and spatial evolution of rifting. **a**, Conceptual models for the different phases of extension based on observations from the Alpine and Iberia/Newfoundland margins. They are set apart by different styles of deformation. The stretching mode (A) is characterized by listric faulting and a differential subsidence of half-grabens exemplified by the Monte Generoso basin[12]. The thinning mode (B) is the least documented of the modes but it can be characterized by maximum thinning of the lithosphere and the presence of a major ductile shear zone (Pogallo shear zone[21]) accommodating differential motion (up to 10 km upward) between the upper crust and the lower crust/upper mantle. It is accompanied by not much uplift of the rift flanks and subsidence in the hanging wall. The exhumation mode (C) is well documented and distinguished by the exhumation of serpentinized upper mantle from less than 10 km depth along a downward-concave fault. **b**, Modelled evolution during lithospheric extension. The plastic strain (brittle deformation) and viscosity field are plotted for the different phases of the modelled evolution of the lithosphere. Note the similarity between the observed and modelled structures. The stress envelope is plotted for a given depth profile (dashed lines for 36 km of extension). For each viscosity field the Mohorovic boundary is shown by a white line. The letter H indicates the hanging block discussed in the main text. **c**, Schematic representation of the temporal and spatial evolution of the three consecutive phases of rifting leading to break-up and seafloor spreading.

delocalization of deformation. In addition to the elastic resistance of the gabbroic lower crust, cooling of the mantle augments the mechanical strength of the lithosphere (A in Fig. 2b). This strengthening in conjunction with viscous flow in the weakened middle crust allows for the distribution of the deformation across the model. The middle crust then forms a 5–6 km decoupling, weak viscous layer composed of DSZs below the block labelled H (for hanging) in Fig. 2b. After 50 km of extension, brittle deformation in the upper mantle leads to the formation of a narrow rift zone below the hanging block H (B in Fig. 2b). Brittle normal faults in the mantle and in the upper crust are decoupled, and form a system of rolling hinge faults on both sides of block H (B in Fig. 2b). In the upper crust, normal faults accommodate large offsets (>30 km), and these thin the crust by exhuming the middle crust and shearing off both sides of block H (B in Fig. 2b). The same motion is accommodated in the mantle, resulting in the exhumation and juxtaposition of deeper mantle levels against middle-crustal rocks. It also leads to the omission of the strong lower crust and upper mantle at the surface. In this 'thinning' mode, the crust can be thinned to less than 10 km depth over distances of over 100 km on both sides of block H (C in Fig. 2b). Coupling of the upper crust and mantle occurs when the low viscosity layer below block H is thinned to less than 4 km. At that point, a robust serpentinite front develops at temperatures below 600 °C (right side of block H; C in Fig. 2b) and at depths of less than 10 km. The faults in the brittle mantle and crust on the right side of block H merge to form one downward concave fault that exhumes the serpentinized mantle at the surface (C in Fig. 2b). The resulting 'transitional' crust formed by exhumation of the middle crust and upper mantle spans a distance of over 100 km and is topped by detachment surfaces (C in Fig. 2b). This system sets up the structure of ocean continent transition (C in Fig. 2a).

The discovery of three consecutive phases of continental extension overprinting each other implies that, in a propagating rift system, these phases must be acting next to each other (Fig. 2c). Thus, we should see distributed listric faulting ahead of propagating rifts (stretching phase A). This distributed listric faulting is then later overprinted by localized detachment faulting that first exhumes the middle crustal levels (thinning phase B) and before exhuming the serpentinized mantle (exhumation phase C). Final break-up then propagates across the rift sequence and separates the margins, leading to seafloor spreading. Such a progression is observed in 'V'-shaped basins, such as the Woodlark basin, for instance[27].

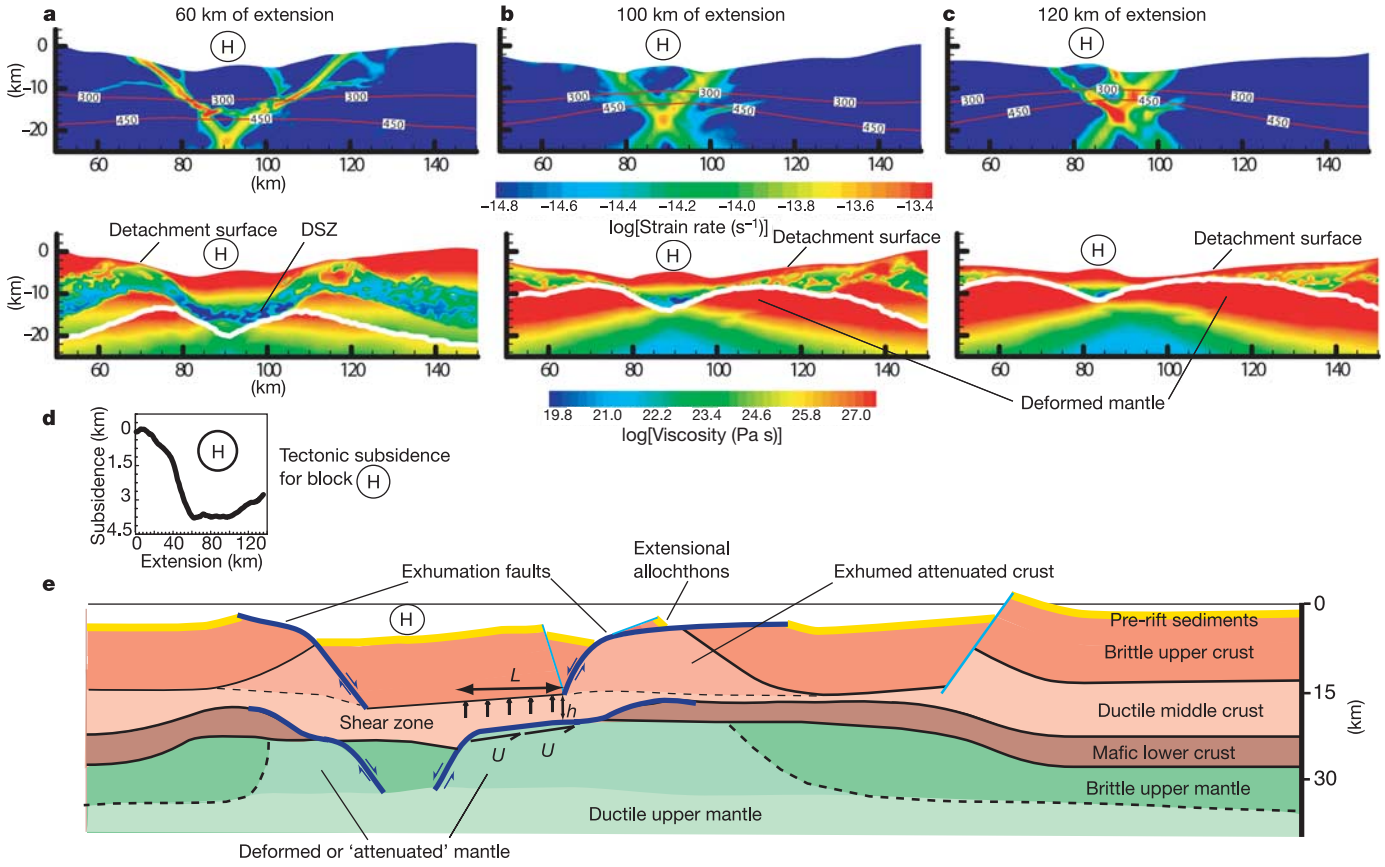

Figure 3 | Details of the modelled thinning phase and conceptual model of crustal thinning. **a**–**c**, Localized deformation during the thinning phase around the block labelled H. Viscous and strain-rate fields for 60 km (**a**), 100 km (**b**) and 120 km (**c**) of extension. The DSZ behaves as a lubricant between block H and the upper mantle. Block H is trapped between two active shear zones. A low-viscosity layer (between 300 °C and 450 °C) corresponds to the DSZ and is dragged at about half of the rifting rate by the motion generated by the DSZ in the mantle. Similar to the flow of a slider-bearing, flow in the DSZ is confined below and around block H. Shear in the DSZ generates a pressure change Q that can support a normal load. Using a low-Reynolds-number approximation: $Q = \eta UL/h^2$, where η is the average viscosity, U is the dragging velocity, L is the length and h is the thickness of the DSZ. For η varying between 10^{19} and 10^{21} Pa s, Q is of the order of a few to tens of MPa. This pressure change can suppress the subsidence of block H during thinning by a few 100 m to 1 km. **d**, This effect may explain why the subsidence of block H is constant during the thinning phase (60–110 km of extension). If the stresses exerted by the DSZ are larger than the yield stress at the base of block H, they may provide the necessary work to thin the crust. This mechanism may explain the formation of extensional allochthons. Finally, the subsidence curve shows that block H is uplifted during the final phase of break-up. This can be explained by the upward-restoring force, resulting in deep necking below the Mohorovic depth in the last phase of rifting[33]. **e**, Conceptual model for the thinning phase during continental break-up. We note that thinning is accommodated by the simultaneous exhumation of middle crust and upper mantle.

Our modelling highlights a new mechanism for lithospheric thinning that can reproduce the major observations made at the Iberia/Newfoundland and Alpine Tethys margins, and evolves from distributed and decoupled stretching phase to a final, localized and coupled, exhumation phase. We find two processes that are likely to weaken the lithosphere and may explain the evolution of rifting: (1) attenuation of the middle crust in the initial stage of rifting, and, (2) serpentinization of the lithosphere during the last exhumation phase. Serpentinization is a critical mechanism to the establishment of a concave-downward fault, because it allows for the weakening of the lithosphere as it bends upward through the rolling hinge. It also replaces the formation of sub-horizontal ductile shear zones as the mechanism that weakens the lithosphere during exhumation. Mid-crustal weakening and serpentinization allow for thinning and exhumation of an originally strong mantle. The presence of an inherited gabbroic lower crust initially leads to distributed thinning in the presence of a weakened middle crust.

The model suggests that exhumation of middle crustal rocks occurs simultaneously with lower crust/mantle thinning along concave, downward faults (Fig. 3 legend). Exhumation leads to the formation of new tectonic surfaces (detachment surfaces) and the lack of rifted crust or pre-rift sediment in the area of continental break-up. This leaves us with no 'seismically detectable' indicator of the amount of strain incurred during thinning. This process may explain poorly understood observations of tectonic subsidence in the absence of observable deformation in the upper crust at other margins (for example, the South Atlantic margin[2–23]). The inferred rheological evolution of the lithosphere shows that weakening is acting to minimize the force that is needed to bend the crust and upper mantle by decoupling them throughout the rift history[28]. In the absence of magmatic activity to weaken the lithosphere, the numerical experiments point to these two processes as key mechanisms allowing continental break-up in a strong lithosphere.

Received 13 October 2005; accepted 24 January 2006.

1. Vening-Meisnez, F. A. Les grabens Africains résultants de compression ou de tension de la croûte terrestre? *Mém. Inst. R. Colon. Belge* **21,** 539–552 (1950).
2. Karner, G. D., Driscoll, N. W. & Barker, D. H. N. in *Petroleum Systems and Evolving Technologies in African Exploration and Production* (eds Arthur, T., MacGregor, D. & Cameron, N. R.). *Spec. Publ. Geol. Soc. Lond.* **207**, 105–129 (2003).
3. Whitmarsh, R. B., Manatschal, G. & Minshull, T. A. Evolution of magma-poor continental margins from rifting to sea-floor spreading. *Nature* **413,** 150–154 (2001).
4. Manatschal, G. New models for evolution of magma-poor rifted margins based on a review of data and concepts from West Iberia and the Alps. *Int. J. Earth Sci.* **93,** 432–466 (2004).
5. Decandia, F. A. & La Elter, P. "Zona" ofiolitifera del Bracco nel settore compreso fra Levanto e la Val Graveglia (Appennino ligure). *Mem. Soc. Geol. Ital.* **11,** 503–530 (1972).
6. Boillot, G. *et al.* Tectonic denudation of the upper mantle along passive margins: A model based on drilling results (ODP Leg 103, western Galicia margin, Spain). *Tectonophysics* **132,** 335–342 (1987).
7. Froitzheim, N. & Eberli, G. P. Extensional detachment faulting in the evolution of a Tethys passive continental margin, eastern Alps, Switzerland. *Geol. Soc. Am. Bull.* **102,** 1297–1308 (1990).
8. Reston, T. J., Krawczyk, C. M. & Hoffmann, H. J. in *The Tectonics, Sedimentation and Palaeoceanography of the North Atlantic Region* (eds Scrutton, R. A., Stoker, M. S., Shimmield, G. B. & Tudhope, A. W.) *Geol. Soc. Spec. Publ.* **90**, 93–109 (1995).
9. Müntener, O., Hermann, J. & Trommsdorff, V. Cooling history and exhumation of lower-crustal granulite and upper mantle (Malenco, eastern central Alps). *J. Petrol.* **41,** 175–200 (2000).
10. Huismans, R. & Beaumont, C. H. Symmetric and asymmetric lithospheric extension; relative effects of frictional-plastic and viscous strain softening. *J. Geophys. Res.* **108**, 10.1029/2002JB002026 (2003).
11. Handy, M. R. Deformation regimes and the rheological evolution of fault zones in the lithosphere: the effects of pressure, temperature, grain size and time. *Tectonophysics* **163,** 119–152 (1989).
12. Bertotti, G. Early Mesozoic extension and Alpine shortening in the western Southern Alps: The geology of the area between Lugano and Menaggio (Lombardy, northern Italy). *Mem. Sci. Geol. (Padova)* **43,** 17–123 (1991).
13. Rutter, E. H., Brodie, K. H. & Evans, P. J. in *The Geometry of Naturally Deformed Rocks* (eds Casey, M., Dietrich, D., Ford, M., Watkinson, J. & Hudleston, P. J.) *J. Struct. Geol.* **15**, 647–662 (1993).
14. Hirth, G. & Tullis, J. Dislocation creep regimes in quartz aggregates. *J. Struct. Geol.* **14,** 145–159 (1992).
15. Rutter, E. H. & Brodie, K. H. in *Continental Lower Crust* (eds Fountain, D. M., Arculus, R. J. & Kay, R. W.) 201–267 (Elsevier, New York, 1992).
16. Fricke, H. C., Wickham, S. M. & O'Neil, J. R. Oxygen and hydrogen isotope evidence for meteoric water infiltration during mylonitization and uplift in the Ruby Montains-East Humboldt Range core complex, Nevada. *Contrib. Mineral. Petrol.* **111,** 203–221 (1992).
17. White, S. H., Burrows, S. E., Carreras, J., Shaw, N. D. & Humphreys, F. J. On mylonites in ductile shear zones. *J. Struct. Geol.* **2,** 175–187 (1980).
18. Jordan, P. The rheology of polymineralic rocks—an approach. *Geol. Rundsch.* **77,** 285–294 (1988).
19. Gilbert, L. E., Scholz, C. H. & Beavan, J. Strain localization along the San Andreas Fault; consequences for loading mechanisms. *J. Geophys. Res.* **99,** 23975–23984 (1994).
20. Tankard, A. J., Welsink, H. J. & Jenkins, W. A. M. in *Extensional Tectonics and Stratigraphy of the North Atlantic Margins* (eds Tankard, A. J. & Balkwill, H. R.) *Am. Assoc. Petroleum Geol. Mem.* **46**, 265–282 (1989).
21. Handy, M. R. & Zingg, A. The tectonic and rheological evolution of an attenuated cross section of the continental crust: Ivrea crustal section, southern Alps, northwestern Italy and southern Switzerland. *Geol. Soc. Am. Bull.* **103,** 236–253 (1991).
22. Pérez-Gussinyé, M., Ranero, C. R., Reston, T. J. & Sawyer, D. Mechanisms of extension at non-volcanic margins: Evidence from the Galicia interior basin, west of Iberia. *J. Geophys. Res.* **108**, 10.1029/2001JB000901 (2003).
23. Contrucci, I. *et al.* Deep structure of the West African continental margin (Congo, Zaïre, Angola), between 5°S and 8°S, from reflection/refraction seismics and gravity data. *Geophys. J. Int.* **158,** 529–553 (2004).
24. Ingebritsen, S. E. & Manning, C. E. Geological implications of a permeability-depth curve for the continental crust. *Geology* **27,** 1107–1110 (1999).
25. Poliakov, A. N. B., Podladchikov, Y. & Talbot, C. Initiation of salt diapirs with frictional overburdens—numerical experiments. *Tectonophysics* **228,** 199–210 (1993).
26. Taylor, B., Goodliffe, A. M. & Martinez, M. How continents break up: Insights from Papua New Guinea. *J. Geophys. Res.* **104,** 7497–7512 (1999).
27. McNutt, M. K., Diament, M. & Kogan, M. G. Variations of elastic plate thickness at continental thrust belts. *J. Geophys. Res.* **93,** 8825–8838 (1988).
28. Lavier, L. L. & Buck, W. R. Half-graben vs. large-offset low-angle normal fault: The importance of keeping cool during normal faulting. *J. Geophys. Res.* **107**, doi:10.1029/2001JB000513 (2002).
29. Escartín, J., Hirth, G. & Evans, B. Effects of serpentinization on the lithospheric strength and the style of normal faulting at slow-spreading ridges. *Earth Planet. Sci. Lett.* **151,** 181–190 (1997).
30. Brace, W. F. & Kohlstedt, D. L. Limit on lithospheric stress imposed by laboratory experiments. *J. Geophys. Res.* **85,** 6248–6252 (1995).
31. Shelton, G. & Tullis, J. A. Experimental flow laws for crustal rocks. *Trans. Am. Geophys. Union* **62,** 396 (1981).
32. Goetze, C. The mechanisms of creep in olivine. *Phil. Trans. R. Soc. Lond.* **288,** 99–119 (1978).
33. Braun, J. & Beaumont, C. in *Sedimentary Basins and Basin-Forming Mechanisms* (eds Beaumont, C. & Tankard, A.) *Can. Soc. Petrol. Geol. Mem.* **12**, 241–258 (1987).

Acknowledgements We thank O. Müntener, G. Péron-Pinvidic, H. Van Avendonk, W. Powell and N. Bangs for help with preparation of the manuscript. We thank T. J. Reston for comments on the manuscript. G.M. was funded by a grant from the programme 'GDR Marge'. L.L.L. was supported by a grant from ExxonMobil Upstream Research Company.

Author Information Reprints and permissions information is available at npg.nature.com/reprintsandpermissions. The authors declare no competing financial interests. Correspondence and requests for materials should be addressed to L.L.L. (luc@ig.utexas.edu).